Seismic Damage Assessment and Soft-Story Response Mechanisms in a Reinforced Concrete Mid-Rise Building Following a Doublet Earthquake Sequence

Lessons Learned for Post-Earthquake Structural Assessment and Seismic Resilience

June 24, 2026 | Venezuela Seismic Event

Authors:

Selen Shojaee
Senior Architectural & Building Energy Specialist

Architectural Systems, Energy Analysis, Building Systems Analysis, Seismic Response, and Resilience Assessment
selen@newschool.edu
https://orcid.org/0009-0004-0518-0239

Ali Abadi
Senior Structural Engineering Specialist

Structural Seismic Assessment & Failure Analysis
aliabadi.ace@gmail.com
https://orcid.org/0009-0005-3596-0065

July 2026 | Technical Report

DOI: https://doi.org/10.5281/zenodo.21663838

Executive Summary

This technical report presents a preliminary structural engineering assessment of the vertically distributed seismic damage observed in a reinforced concrete frame building documented following the June 24, 2026 Venezuela earthquake sequence that was characterized by the U.S. Geological Survey (USGS) as a doublet earthquake, consisting of an M7.2 foreshock followed approximately 39 seconds later by an M7.5 mainshock (U.S. Geological Survey [USGS] 2026).

In the absence of in-person site access and without availability of original structural drawings, construction documents, or material test data, this assessment relies exclusively on publicly available occupant-recorded video footage captured during emergency egress.

The exact geographic location of the investigated structure was not publicly disclosed; therefore, regional earthquake parameters are used solely to provide seismic context and are not interpreted as building-specific ground-motion demands.

Applying established seismic evaluation principles from ASCE 7-22, ASCE 41-17, ACI 318-19, and FEMA 306 (ASCE 41-17, 2017; ASCE 7-22, 2022; ACI 318, 2019; FEMA 306, 1998), the analysis examines potential soft-story behavior, the apparent vertical distribution of damage, and the potential contribution of unreinforced masonry infill walls to the structural response. The findings indicate an apparent vertical damage gradient, progressing from localized upper-story cracking to extensive ground-story infill distress and localized failure characteristics.

The ground floor exhibited deformation patterns consistent with a potential soft-story stiffness discontinuity and an apparent concentration of deformation demand. Unreinforced masonry infills likely contributed to lateral stiffness and exhibited damage patterns associated with brittle in-plane shear and out-of-plane failure mechanisms. Despite this severe infill damage, visual evidence did not indicate global collapse or loss of primary frame stability.

Furthermore, the sequence suggests a plausible foreshock-mainshock interaction hypothesis, wherein the initial event may have contributed to localized pre-damage, stiffness degradation of vulnerable infills, and increased susceptibility to further damage, potentially contributing to increased damage severity during the mainshock (VERT 2026). This study demonstrates the value of video-based engineering assessment under limited post-earthquake data conditions and presents bounded engineering

hypotheses while prioritizing physical inspections, rapid visual screening for comparable reinforced concrete typologies, and enhanced consideration of infill-frame interaction effects in future seismic assessments.

Table of Contents

List of Figures

List of Tables

1. Introduction

1.1 Background

Reinforced concrete (RC) frame buildings with unreinforced masonry (URM) infill walls represent a widely deployed construction typology in seismically active regions. Although historically treated as nonstructural elements in conventional design, URM infills can significantly alter the global lateral stiffness, mass distribution, and load paths of structural systems (Paulay and Priestley, 1992; FEMA 306, 1998). Numerous experimental and analytical investigations have confirmed that intact infill panels increase lateral stiffness and modify force-transfer mechanisms during the early stages of ground shaking, while simultaneously introducing brittle failure mechanisms and irregular structural response (Crisafulli 1997; Dolšek and Fajfar 2008). The complex interaction between RC frames and masonry infill walls can produce localized response irregularities, including soft-story irregularities and brittle in-plane shear or out-of-plane failure mechanisms, particularly where infill distribution varies along the height of a building. Evaluating these interdependent failure modes during post-earthquake reconnaissance remains a critical challenge for structural engineers.

Post-earthquake reconnaissance following major seismic events has repeatedly documented this vulnerability. Field investigations conducted after the 1994 Northridge earthquake and the 1995 Hyogo-ken Nanbu (Kobe) earthquake reported extensive infill damage, concentrated inter-story deformation, and nonstructural failures even where the primary RC framing system remained standing (EERI 1995; EERI, 1996). These precedents demonstrate that infill damage can significantly affect building functionality, life-safety performance, and post-earthquake repair requirements independent of global structural collapse. The economic and engineering implications of soft-story response and retrofit requirements for RC frame buildings have also been documented in previous analytical studies (Agha Beigi et al., 2015).

Immediate physical access to earthquake-damaged structures is frequently restricted due to safety hazards, regulatory cordons, or logistical constraints. Under such data-scarce conditions, alternative sources of evidence — most notably occupant-recorded video documentation — provide valuable information regarding observed structural and nonstructural response, particularly when integrated with established principles of structural mechanics and performance-based seismic evaluation (FEMA 306, 1998; FEMA P-58-1, 2018). This report follows that evidence-based approach.

In this investigation, occupant-recorded video documentation was treated as observational evidence and interpreted through established structural engineering principles.

1.2 Objective and Scope of the Study

The June 24, 2026 Venezuela earthquake sequence, consisting of an M7.2 foreshock followed approximately 39 seconds later by an M7.5 mainshock, generated severe shaking across the north-central coast of Venezuela and the Caracas metropolitan region (USGS 2026; VERT 2026). Because immediate physical access was precluded by both geographical distance and the severe post-earthquake safety hazards at the site, this study utilizes occupant-recorded video documentation captured during emergency evacuation to assess the apparent spatial distribution of seismic damage in a single multi-story RC frame building. The exact geographic location of the investigated building was not publicly disclosed; consequently, the present assessment emphasizes observed damage characteristics rather than site-specific seismic demand estimation.

The primary objective of this technical case study is to present an evidence-based preliminary evaluation of the observed damage patterns in the subject building. By interpreting observed damage indicators within the framework of established seismic design and evaluation principles — including ASCE 7-22 (2022), ASCE 41-17 (2017), ACI 318-19 (2019), and FEMA 306 (1998) — this report aims to identify plausible damage mechanisms, evaluate the structural implications of URM infill participation, and establish a baseline for further analytical modeling and subsequent engineering assessments and future seismic resilience strategies.

1.3 Relevance to U.S. Seismic Practice

Although this investigation examines a seismic event outside the United States, the evaluated failure mechanisms are directly relevant to seismic risk reduction practices in U.S. building stock. Soft-story behavior, masonry infill–frame interaction, and drift-sensitive nonstructural component damage represent recurring challenges in seismic performance assessment and resilience planning. Accordingly, the observations and analytical framework presented in this report provide transferable insights applicable to seismic evaluation, retrofit prioritization, and post-earthquake recovery strategies within the United States.

1.4 Report Organization

The remainder of this report is organized as follows: Section 2 summarizes the earthquake event, available evidence, and investigation methodology; Section 3 presents observed structural damage characteristics; Section 4 provides structural interpretation and code-based analysis; Section 5 presents contributing factors and the failure hypothesis; Section 6 discusses limitations and scope of evaluation; Section 7 presents conclusions; and Section 8 provides recommendations.

2. Earthquake Event, Evidence, and Investigation Methodology

2.1. Overview of the June 24, 2026, Earthquake Sequence

The June 24, 2026, earthquake sequence in Venezuela consisted of an M7.2 foreshock followed approximately 39 s later by an M7.5 mainshock (USGS 2026). The short interval between the two events may have influenced the subsequent response of the investigated building, particularly if damage accumulated during the initial ground motion (VERT 2026). Damage potentially sustained during the foreshock may have altered the stiffness and deformation characteristics of susceptible structural and nonstructural components before the mainshock, thereby influencing their subsequent response. This earthquake sequence provides the basis for the present technical assessment, which focuses on the observed damage patterns within a single reinforced concrete frame building.

Table 1: Summary of Regional Seismic Parameters and Investigation Context

Parameter	Technical Details
Seismic Sequence	M 7.2 Foreshock / M 7.5 Mainshock (39s apart)
Epicenter	10.436°N, 68.528°W-Foreshock/10.509°N, 68.504°W-Mainshock
Epicentral Region	Near Yumare, Venezuela
Ground Motion (PGA/PGV)	PGA: 0.786 g; PGV: 86.26 cm/s (USGS 2026 ShakeMap regional estimate)
Intensity & Site Class	MMI IX (Violent) / Regional Site Class B (Hard rock) (Vs30: 760–800 m/s)
Evidence Source	Publicly available occupant-recorded video captured during emergency egress

2.1.1 Interpretation of Regional Seismic Parameters

The seismic parameters summarized in Table 1 represent regional earthquake characteristics and are used solely to establish the severity and context of the seismic event. Because the exact geographic location of the investigated structure was not publicly disclosed, these values are not interpreted as building-specific seismic demand parameters.

2.2. Available Evidence

Standard post-earthquake investigations typically rely on direct access to damaged structures, field measurements, visual inspections, photographic documentation, and engineering reconnaissance conducted at the affected site. In the present case, direct on-site access to the investigated building was not available; therefore, the assessment was performed remotely using available observational evidence associated with the earthquake sequence.

Consequently, this assessment relies primarily on occupant-recorded video footage captured during emergency evacuation. Although such footage does not provide quantitative information such as structural dimensions, material properties, or measured seismic response data, it provides qualitative information regarding damage distribution, deformation patterns, and the progression of observed structural and nonstructural damage. All observations presented in this study are therefore limited to features directly visible in the available video record, and interpretations are intentionally confined to evidence that can be reasonably supported by established principles of structural mechanics.

2.3. Investigation Methodology

The assessment methodology consisted of three primary components. First, the video footage was examined to document the apparent distribution of damage throughout the height of the structure and to identify visible indicators of cracking, deformation, and infill wall distress. Observations from different segments of the video were reviewed to maintain consistency in damage interpretation.

Second, the structural system was characterized using observable architectural and structural features because original design drawings and structural documentation were unavailable. Based on visible framing characteristics and wall configurations, the building was interpreted as a reinforced concrete (RC) frame building with unreinforced masonry (URM) infill walls.

Finally, the observed damage characteristics were interpreted using established seismic design and evaluation principles, including seismic evaluation concepts from ASCE 7-22, ASCE 41-17, ACI 318-19, and FEMA 306. No analytical or numerical structural modeling was performed because the information required to develop and validate a reliable structural model was unavailable. The assessment is therefore limited to a qualitative interpretation of the documented structural response, with particular emphasis on potential soft-story behavior, frame–infill interaction effects, and the apparent progression of damage throughout the earthquake sequence.

3. Observed Damage Characteristics and Preliminary Performance-Level Interpretation

The following damage observations are based exclusively on video stills extracted from occupant-recorded footage obtained during the June 24, 2026 seismic sequence. Observations are limited to stairwell and corridor areas visible during the occupant's emergency egress. Floor designations are approximate because the total number of stories and the elevation of individual observations could not be independently verified from the available footage.

3.1 Upper Stories: Damage Conditions Consistent with Immediate Occupancy

Video stills captured at the upper story levels did not reveal evidence of significant structural or nonstructural damage. Corridor walls and stairwell enclosures appeared intact, with clean floor surfaces and no visible debris accumulation. A single hairline diagonal crack observed at a wall-to-slab interface represented the only visible feature potentially associated with seismic demand at this level. Door frames appeared to remain plumb, with no visible evidence of significant distortion. These observations were generally consistent with visual damage conditions commonly associated with the

Immediate Occupancy (IO) performance level described in ASCE 41-17, Section 2.3.1.1 and Table 2-3 (ASCE 2017).

Figure 1: Representative condition of upper stories showing intact finishes, minor hairline cracking, and lack of debris accumulation.

3.2 Intermediate Stories: Damage Conditions Consistent with Life Safety

As the occupant descended toward the mid-level floors, video stills documented a progressive increase in damage severity. Diagonal cracking patterns and partial loss of plaster cover were visible at stairwell landing walls, with exposed masonry units consistent with localized in-plane infill distress. Debris accumulation on stair treads increased with each successive landing. Door frames at this level remained largely intact, though minor racking distortion was suggested by gap formation at frame corners. Visible stair structural elements appeared to maintain their overall geometric integrity throughout this zone. These observations were generally consistent with visual damage characteristics commonly associated with the **Life Safety (LS) performance level** described in ASCE 41-17, Section 2.3.1.2 and Table 2-3 (ASCE 2017).

Figure 2: Intermediate story level demonstrating progressive in-plane shear cracking, minor plaster spalling, and initial debris accumulation on stair treads.

3.3 Lower Stories: Severe Damage Conditions Approaching Collapse Prevention

A pronounced escalation in damage severity was observed at the lower story levels. Video stills documented prominent vertical cracking extending over significant portions of the stairwell infill walls, accompanied by large-scale plaster loss and exposed brick units on both wall faces, suggesting out-of-plane instability or loss of continuity within portions of the infill panels. Heavy debris accumulation covered stair treads and landing slabs. Partial breach of stairwell enclosure walls was visible, with daylight penetration through damaged infill panels suggesting substantial loss of wall continuity. These observations were generally consistent with severe nonstructural and infill damage approaching conditions associated with the **Collapse Prevention (CP) performance level** described in ASCE 41-17, Section 2.3.1.3 and Table 2-3 (ASCE 2017); however, the available visual evidence was insufficient to establish the overall structural performance level.

Figure 3: Lower story levels showing severe out-of-plane infill panel distress, large-scale plaster loss, and extensive debris accumulation on landing slabs.

3.4 Ground Level: Severe Damage and Apparent Soft-Story Response

Video stills captured at the ground-floor level documented the most severe damage observed throughout the occupant's descent. Extensive damage and localized loss of masonry infill walls were evident within the visible ground-level areas, with unreinforced masonry units dispersed across floor surfaces and extending to visible exterior areas, consistent with both in-plane shear distress and out-of-plane instability mechanisms. RC frame elements, including visible columns and beams, appeared to have retained their geometric alignment, suggesting an infill-dominated damage pattern rather than visible evidence of global collapse of the RC frame system. Nonstructural systems, including partition walls, ceiling elements, and interior finishes, were extensively damaged.

The observed ground-story infill damage represented severe damage to nonstructural components, with observed conditions approaching damage states associated with extensive nonstructural damage conditions described in ASCE 41-17, Section 2.3.1.3 and Table 2-3 (ASCE 2017); however, the apparent integrity of visible RC frame members precluded a definitive assessment of the primary structural performance level based solely on available visual evidence. The occupant's descent was obstructed at the basement stair entry, which was found impassable due to debris accumulation, preventing visual assessment of below-grade conditions.

Table 2 summarizes the preliminary damage interpretation based on visible observations. These classifications represent qualitative comparisons with ASCE 41-17 performance-level descriptions and do not constitute a formal structural performance evaluation (ASCE 2017).

Figure 4: Ground-floor level and basement stair entry showing near-total masonry infill failure, heavy structural debris obstruction, and standing water from damaged MEP utilities.

Table 2: Summary of Observed Damage States by Building Level

Building Level	Primary Observations	Implied ASCE 41-17 Level (ASCE 2017)
Upper Stories	Hairline cracking, no debris, intact finishes and doors	Immediate Occupancy (IO)
Intermediate Stories	Diagonal shear cracking, partial infill loss, moderate debris	Life Safety (LS)
Lower Stories	Vertical cracking, out-of-plane failure, heavy debris	Collapse Prevention (CP)
Ground Level	Near-total infill loss, visible RC frame alignment maintained, exterior brick dispersion	Severe nonstructural damage; structural performance not confirmed
Below Grade	Inaccessible - debris obstruction at stair entry	Not Assessed

4. Structural Mechanics and Code-Based Analysis

4.1 Lateral Force Distribution and Base Shear Accumulation

Under ASCE 7-22 Section 12.8.3, the design lateral seismic force at story level i in an equivalent lateral force (ELF) procedure is distributed proportionally to the product of story weight and height raised to the power k, where k depends on the fundamental period T of the structure (ASCE 2022).

ASCE 7-22 Section 12.8.3—Lateral Force Distribution (ASCE 2022):

$$F_x = C_{vx}V \qquad \text{Eq. (1)}$$

$$C_{vx} = \frac{w_x h_x^k}{\sum_{i=1}^{n} w_i h_i^k} \qquad \text{Eq.(2)}$$

where C_{vx} = Vertical distribution factor;

V = Total design lateral force or shear at the base of the structure [kip (kN)];

w_i , w_x = Portion of the total effective seismic weight of the structure (W) located or assigned to level i or x;

h_i , h_x = Height [ft (m)] from the base to level i or x;

k = Exponent related to the structure period as follows:

For structures that have a period of 0.5 s or less, k = 1;

for structures that have a period of 2.5 s or more, k = 2; and

for structures that have a period between 0.5 and 2.5 s, k shall be 2 or shall be determined by linear interpolation between 1 and 2.

A direct consequence of this distribution is that the design lateral force assigned to individual stories generally increases with elevation, reaching its largest value at the uppermost story.

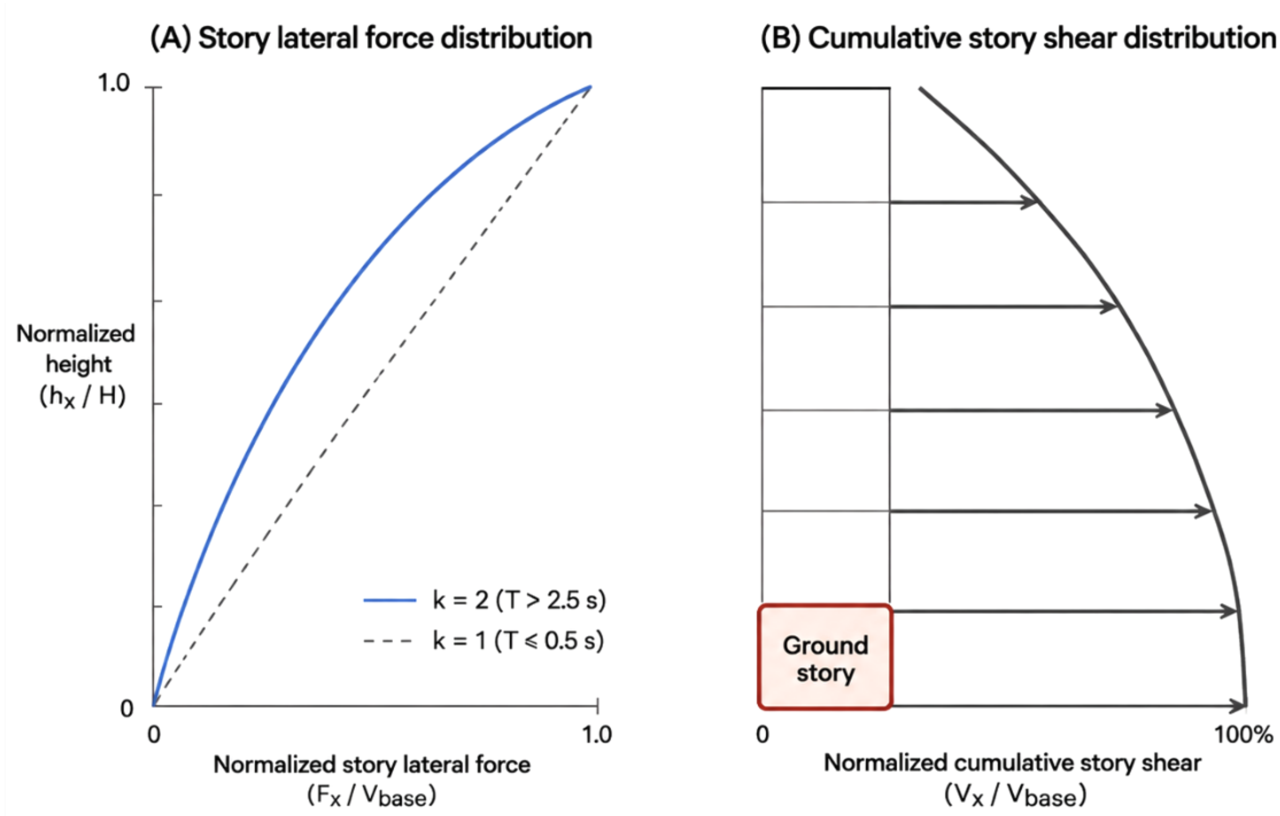

Figure 5: Conceptual relationship between equivalent lateral force distribution and cumulative story shear demand in a multi-story RC building (based on ASCE 2022).

Although the lateral force assigned to individual stories increases toward the roof, the cumulative story shear increases progressively toward the base as the sum of all lateral forces acting at and above the story under consideration (ASCE 2022).

$$V_x = \sum_{i=x}^{n} F_i \qquad \text{Eq.(3)}$$

where F_i is the portion of the seismic base shear, V [kip (kN)], induced at level i.

Accordingly, the distribution of cumulative story shear differs from the distribution of individual story forces.

$$V_{ground} = V_{base} = \sum_{i=x}^{n} F_i = 100\% \text{ of total seismic base shear} \qquad \text{Eq.(4)}$$

This relationship explains why the highest cumulative shear demand develops at the ground story. The columns, walls, and lateral force-resisting elements at the ground story must simultaneously resist the cumulative shear force transferred from every story above, while also developing the maximum overturning moment at the base of the structure. Accordingly, the ground story is subjected to the highest combination of cumulative shear, overturning moment, and axial force variation within the structural system.

Relation Between Base Shear Distribution and Observed Damage

The observed vertical distribution of damage presented in Section 3 is consistent with the cumulative story shear distribution described above. Upper stories, despite potentially experiencing greater dynamic amplification effects, are subjected to relatively lower cumulative story shear demands — consistent with the minimal damage (IO level) observed in video stills at those levels. As the occupant descended, each successive story level sustained progressively higher cumulative shear, corresponding directly to the progressive escalation in observed damage severity.

It is important to note that the ELF-based force and cumulative shear distributions described above represent an idealized, static approximation of seismic demand and do not fully capture the dynamic, nonlinear response of the structure during an actual earthquake. Higher-mode contributions, floor acceleration amplification, and transient dynamic effects (sometimes informally referred to as a whiplash effect) can produce localized demand concentrations at upper stories that are not predicted by the triangular ELF distribution alone. Consequently, while the cumulative story shear framework provides a plausible and code-consistent explanation for the observed damage gradient, it should be understood as one contributing mechanism among several, rather than a complete or exclusive explanation of the observed response. A more rigorous assessment of the relative contribution of static force distribution versus dynamic amplification effects would require nonlinear response history analysis, which is beyond the scope of the available evidence in this study.

At the ground story, where V_{base} was resisted entirely by the ground-floor structural system, the combination of maximum cumulative shear demand, soft-story stiffness concentration (Section 4.2), and unreinforced masonry infill brittleness (Section 4.3) are consistent with the severe nonstructural damage documented in Section 3.4.

The influence of cumulative story shear should be considered independently of the soft-story irregularity discussed in Section 4.2. Even in a structurally regular building without stiffness discontinuity, the ground story would sustain the maximum shear demand. In the subject structure, the soft-story condition amplified this inherent vulnerability by further concentrating inter-story drift at the ground level, contributing to a compounding failure mechanism in which maximum force demand and maximum deformation demand coincided at the same story.

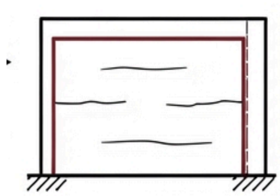

Upper stories

Hairline cracking, no debris

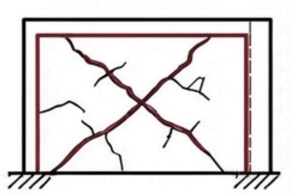

Intermediate stories

Diagonal shear cracking

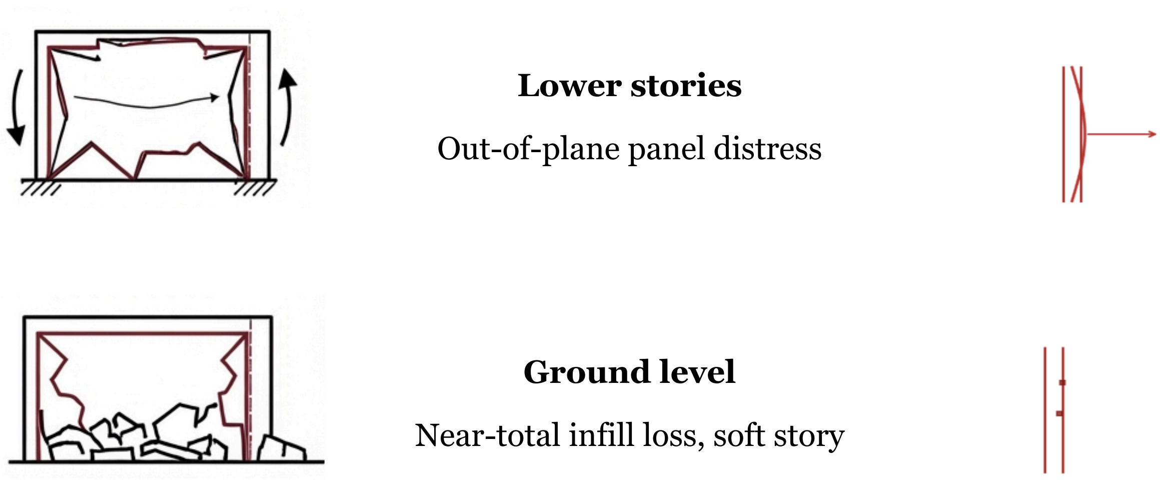

Figure 6: Conceptual relationship between story level, cumulative seismic demand, and observed infill damage progression (based on ASCE 2022).

4.2 Soft-Story Irregularity (ASCE 7-22 §12.3.2.2)

Under ASCE 7-22 Section 12.3.2.2, a soft-story irregularity is defined as a condition in which the lateral stiffness of a given story is less than 70 percent of the lateral stiffness of the story above, or less than 80 percent of the average lateral stiffness of the three stories above (ASCE 2022). In RC moment-resisting frame buildings with masonry infill walls, this condition frequently results from architectural requirements in which the ground floor is left open or sparsely infilled to accommodate commercial, parking, or lobby functions, while upper stories appear to contain more continuous infill distributions. The resulting stiffness discontinuity concentrates seismic-induced lateral deformation demand at the soft story, subjecting the story columns to substantially increased inter-story drift demands.

Table 3: ASCE 7-22 Table 12.3-1 Stiffness Irregularity Classification Criteria (ASCE 2022)

Type	Description
1a	**Stiffness–Soft Story Irregularity** is defined to exist where there is a story in which the lateral stiffness is less than 70% of that in the story above or, where there are at least three stories above, less than 80% of the average stiffness of the three stories above.
1b	**Stiffness–Extreme Soft Story Irregularity** is defined to exist where there is a story in which the lateral stiffness is less than 60% of that in the story above or, where there are at least three stories above, less than 70% of the average stiffness of the three stories above.

The stiffness irregularity criteria defined in ASCE 7-22 Table 12.3-1 can be expressed as follows:

Type 1a — Soft Story: $K_i < 0.70\ K_{i+1}$ Eq.(5)

or, where three stories exist above: $K_i < 0.80\ (K_{i+1} + K_{i+2} + K_{i+3})/3$ Eq.(6)

Type 1b — Extreme Soft Story: $K_i < 0.60\ K_{i+1}$ Eq. (7)

or: $K_i < 0.70\ (K_{i+1} + K_{i+2} + K_{i+3})/3$ Eq.(8)

where:

K_i = lateral stiffness of story i

K_{i+1} = lateral stiffness of the story immediately above

For buildings assigned to applicable seismic design categories, the presence of extreme stiffness irregularity may affect the permitted analysis procedures in accordance with ASCE 7-22 §12.3.3.1 (ASCE 2022).

The damage pattern documented in Section 3 is consistent with this mechanism. The near-total loss of infill walls at the ground level, juxtaposed with the progressive retention of infill integrity at intermediate and upper stories, suggests that the ground story likely experienced the highest concentration of lateral deformation demand during the June 24, 2026 seismic sequence.

The concentration of lateral deformation demand associated with a soft-story condition is evaluated through inter-story drift response. Although actual drift values cannot be determined from the available video evidence, the observed damage pattern is consistent with elevated ground-story deformation demand and associated masonry infill degradation.

4.3 Masonry Infill Walls: Unintended Structural Contribution and Failure Modes

Masonry infill walls in RC frame buildings are conventionally classified as nonstructural elements and are typically excluded from lateral force-resisting system design under both ASCE 7-22 and ACI 318-19 (ASCE 2022; ACI 2019). However, their inherent in-plane stiffness—often substantially greater than that of the surrounding RC frame—causes them to attract and resist seismic lateral forces prior to failure, thereby modifying the overall lateral response of the structural system. This unintended structural interaction has two principal consequences: it alters the building's dynamic characteristics, and it introduces brittle failure modes absent from the design basis.

Masonry infill walls exhibit two distinct failure modes under seismic loading. In-plane failure occurs when lateral forces parallel to the wall plane induce diagonal shear cracking, typically propagating from corner to corner in an X-pattern, followed by progressive crushing of compression struts and loss of load-carrying capacity. Out-of-plane failure occurs when inertial forces perpendicular to the wall plane — amplified by the dynamic response of the infill panel — exceed the wall's flexural and arching capacity, resulting in sudden expulsion of the masonry units from the frame bay. The observed damage patterns are consistent with both failure mechanisms: diagonal shear cracking is observed at intermediate story levels, consistent with in-plane demand, while the near-total expulsion of brick units at the ground level and the presence of exterior debris fields suggest that out-of-plane instability was a significant contributing mechanism at the critical story.

Table 4: Masonry Infill Wall Failure Modes and Observed Evidence (adapted from Paulay and Priestley 1992; FEMA 1998)

Failure Mode	Seismic Force Direction	Crack Pattern	Stage of Failure	Observed in This Investigation
In-Plane Shear	Parallel to wall plane	Diagonal X-pattern (shear-tension)	Gradual — crack propagation then crushing	Yes — intermediate stories
Out-of-Plane Overturning	Perpendicular to wall plane	Horizontal flexural cracking then expulsion	Sudden — brittle ejection of masonry units	Yes — ground level, exterior debris field

For analytical purposes, masonry infill walls are commonly represented using the equivalent diagonal compression strut model originally developed by Mainstone (1971) and subsequently described in FEMA 306 (Section 7.3) (FEMA 1998,). The effective strut width is expressed as:

$$a = 0.175\,(\lambda_h\, h_{inf})^{-0.4}\, d_{inf} \quad \text{Eq.(9)}$$

Where:

a = effective strut width

h_{inf} = height of the infill panel

d_{inf} = diagonal length of infill panel

λ_h = relative stiffness parameter, calculated per FEMA 306 as:

$$\lambda_h = \sqrt[4]{\frac{E_m\, t\, sin(2\theta)}{4\, E_c\, I_c\, h_{inf}}} \quad \text{Eq.(10)}$$

E_m = modulus of elasticity of the masonry

t = thickness of the infill panel

θ = angle of the diagonal strut with the horizontal

E_c = modulus of elasticity of the frame concrete

I_c = moment of inertia of the confining columns

The effective cross-sectional area of the strut Ae and its axial stiffness K_{strut} follow from FEMA 306 (Section 7.3.2):

$$A_e = a\ .\ t \qquad \text{Eq.(11)}$$

The lateral stiffness of the masonry infill, K_{infill}, is modeled as an equivalent diagonal strut, where the effective stiffness is defined based on the pre-cracking mechanical properties of the panel. The axial stiffness of this strut, K_{strut}, is given by:

$$K_{strut} = \frac{A_e E_m}{D_{infill}} \qquad \text{Eq.(12)}$$

To resolve this stiffness into the horizontal direction, the lateral stiffness contribution of the infill K_{infill} is expressed as:

$$K_{infill} = K_{strut}\ cos^2(\theta) \qquad \text{Eq. (13)}$$

where

A_e = effective cross-sectional area of the strut,

This formulation is applicable to the elastic (pre-cracking) response of the infill panel (FEMA 1998). Following crack initiation, FEMA 306 (FEMA 1998) recommends applying stiffness reduction to represent the progressive nonlinear degradation of wall–frame interaction.

Assuming perfect bond between the RC frame and the masonry infill prior to cracking, the total story stiffness may be approximated as:

$$K_{total} = K_{frame} + K_{infill} \qquad \text{Eq.(14)}$$

As long as the infill remains intact, both the RC frame and the masonry panel contribute to the lateral stiffness of the story. As stiffness degrades, a progressively larger portion of the lateral load is redistributed to the surrounding RC frame members, resulting in increased inter-story drift demand and localized deformation.

4.4 Frame-Infill Interaction and Vertical Damage Concentration

The observed progression of damage severity, from minimal distress at the upper stories to extensive infill damage at the ground level, is compatible with a response mechanism involving soft-story deformation concentration and progressive infill degradation. As the ground-story infill walls experienced progressive degradation during the June 24, 2026 seismic sequence, their contribution to lateral stiffness and force resistance would have progressively diminished. Consequently, a greater portion of the lateral demand would have been transferred to the surrounding RC frame elements. The apparent retention of column geometric integrity suggests that the RC frame redistributed a greater share of the lateral demand without visible evidence of global frame collapse, though this assessment cannot be confirmed without field investigation and evaluation of reinforcement detailing, concrete condition, and member damage in accordance with ASCE 41-17 Chapter 10 (ASCE 2017).

Current design provisions in ASCE 7-22 and ACI 318-19 generally do not require masonry infill walls to be included as primary components of the lateral-force-resisting system (ASCE 2022; ACI 2019). Nevertheless, previous experimental and analytical studies have demonstrated that intact masonry infill panels may significantly influence structural stiffness, lateral load distribution, and inter-story drift prior to cracking. Consequently, the actual seismic response of infilled RC frames may differ from that assumed in conventional code-based design. The observed damage pattern documented in this investigation is compatible with this established frame–infill interaction mechanism, although quantitative evaluation would require detailed structural modeling and field verification beyond the scope of the available visual evidence.

4.5 Global Stiffness Matrix Representation of Ground-Story Infill Degradation

For an n-story shear building, the global stiffness matrix [K] represents the contribution of story stiffness from both the bare RC frame (K_f) and masonry infill (K_{infill}) at each level.

The total lateral stiffness of each story may be expressed as:

$$K_{global} = \sum K_{elements} \quad \text{Eq. (15)}$$

$$K_{total} = K_{frame} + K_{infill} \quad \text{Eq. (16)}$$

When ground-story infill contribution is significantly degraded or idealized as ineffective after failure, K_{infill} approaches zero, introducing a pronounced stiffness discontinuity in the first story.

$$[K] = \begin{bmatrix} (k_{f1}+k_{i1})+(k_{f2}+k_{i2}) & -(k_{f2}+k_{i2}) & 0 & \cdots \\ -(k_{f2}+k_{i2}) & (k_{f2}+k_{i2})+(k_{f3}+k_{i3}) & -(k_{f3}+k_{i3}) & \cdots \\ 0 & -(k_{f3}+k_{i3}) & \cdots & \cdots \\ \vdots & \vdots & \vdots & (k_{fn}+k_{in}) \end{bmatrix} \quad \text{Eq. (17)}$$

$$K_{infill,1} \rightarrow 0 \quad \text{Eq. (18)}$$

This stiffness discontinuity means that under identical lateral loading, the ground story undergoes disproportionately large lateral displacement relative to all other stories. The resulting stiffness discontinuity causes a concentration of lateral deformation demand at the ground story. This mechanism provides a plausible analytical explanation for the observed damage gradient documented in Section 3.

4.6 Seismic Demand on Nonstructural Components (ASCE 7-22 Chapter 13)

The extensive damage to mechanical, electrical, and plumbing (MEP) systems observed at the ground level is directly associated with elevated inter-story drift demand and relative displacement effects (D_p) rather than inertial force effects or story shear alone.

While ASCE 7-22 §13.3.1 defines the seismic design force for the inertial anchorage of nonstructural components as (ASCE 2022):

$$F_p = \left[\frac{0.4\,.\,ap\,.\,sds\,.\,W_p}{\left(\frac{R_p}{I_p}\right)}\right].\left(1 + 2\frac{z}{h}\right) \qquad \text{Eq.(19)}$$

$$\text{Minimum: } F_p \geq 0.3 \cdot SDS \cdot I_p \cdot W_p \qquad \text{Eq. (20)}$$

$$\text{Maximum: } F_p \leq 1.6 \cdot SDS \cdot I_p \cdot W_p \qquad \text{Eq. (21)}$$

where

ap = component amplification factor

SDS = short-period spectral acceleration

W_p = component weight

R_p = component response modification factor

I_p = component importance factor

z = Height in the structure of the component's attachment point with respect to the building base.

h = average roof height of the structure with respect to the base.

Although the $\left(1 + 2\frac{z}{h}\right)$ height amplification factor is minimized at ground level ($z \rightarrow 0$), the soft-story mechanism generated inter-story drift demands that produced relative displacements (Dp) on MEP systems that far exceeded their deformation capacity. Piping systems, electrical conduits, and HVAC ducts without flexible couplings at the ground-floor connections may have experienced brittle tensile, shear, or connection-related damage, consistent with the MEP distress observed in available video stills.

This behavior is consistent with the soft-story mechanism described in Section 4.2, where concentrated inter-story deformation produces amplified relative displacement demands at the ground level.

The observed MEP damage at the ground level is therefore considered consistent with drift-sensitive nonstructural component distress associated with elevated story deformation demand. However, confirmation of specific failure modes would require field inspection of component anchorage, connections, and seismic restraint systems.

5. Contributing Factors and Failure Hypothesis

5.1 Probable Contributing Factors

Based on the damage pattern documented in Section 3 and the structural mechanics outlined in Section 4, several contributing factors are identified as probable contributors to the observed ground-story failure. These factors are advanced as engineering hypotheses informed by visual evidence and code-based reasoning; they cannot be confirmed without physical inspection, structural drawings, and material testing.

5.1.1 Vertical Stiffness Discontinuity at Ground Level

The most significant probable contributing factor is the presence of a pronounced stiffness discontinuity between the ground story and the floors above. The video evidence suggests that upper stories were uniformly infilled, while the ground-floor configuration — whether originally open for lobby use, or subsequently modified — exhibited substantially reduced infill density. Under ASCE 7-22 Section 12.3.2.2 and Table 12.3-1, this condition would classify the structure as possessing a soft-story irregularity of Type 1a or 1b, triggering mandatory analytical and detailing requirements that may not have been implemented in the original design (ASCE 2022).

5.1.2 Absence of Infill-Frame Separation Detailing

In structures where masonry infill walls are intended to function as nonstructural elements, modern seismic design practice recommends the provision of gap detailing at the infill-frame interface to decouple the infill from the lateral force-resisting system (Paulay and Priestley 1992; ASCE 2022). The damage pattern observed, particularly the diagonal shear cracking at intermediate levels and the sudden out-of-plane failure at the ground level, is characteristic of fully contact infill panels without isolation detailing. The absence of such measures would have caused the infill walls to engage the RC frame under lateral loading, introducing the stiffness irregularity and brittle failure modes described in Section 3.

5.1.3 Unreinforced Masonry Construction

The exposed brick units visible throughout the video documentation exhibit no evidence of reinforcement, bed joint reinforcement, or confining elements. Unreinforced masonry infill is particularly susceptible to both in-plane shear failure and out-of-plane expulsion under seismic loading, as it lacks the tensile capacity necessary to redistribute cracking forces or resist inertial demands perpendicular to the wall plane (Paulay and Priestley 1992; FEMA 1998). This observation is consistent with masonry infill construction practices historically used in many reinforced concrete frame buildings in Latin America (Basha and Kaushik 2016; Pallarés et al. 2021; Sleiman et al. 2024); however, confirmation of reinforcement details would require physical inspection.

5.1.4 Cumulative Seismic Demand from Foreshock-Mainshock Sequence

The sequence consisted of a M7.2 foreshock followed approximately 39 seconds later by a M7.5 mainshock, producing repeated high-intensity seismic demand within a short time interval. Regional USGS ShakeMap estimates indicated a peak ground acceleration (PGA) of approximately 0.786 g and a peak ground velocity (PGV) of approximately 86.26 cm/s, reflecting a severe level of regional ground shaking compatible with the widespread structural and nonstructural damage observed throughout the affected area (USGS ShakeMap 2026). These values represent regional ShakeMap estimates and should not be interpreted as site-specific ground motion demands for the subject structure.

The foreshock likely initiated cracking and partial degradation of infill panels at the ground level, reducing their lateral stiffness and load-carrying capacity prior to the arrival of the mainshock (VERT 2026; Sleiman et al. 2024). The mainshock then imposed peak seismic demand on a ground story already compromised by foreshock-induced damage, effectively amplifying the soft-story effect and accelerating infill failure progression. This cumulative demand scenario is consistent with the near-total infill loss observed at the ground level.

5.2 Failure Hypothesis

Synthesizing the observational evidence and contributing factors identified above, the following failure hypothesis is advanced:

The subject building, an RC moment-resisting frame structure with unreinforced masonry infill walls, exhibited a pronounced soft-story condition at the ground level attributable to a vertical stiffness discontinuity between the sparsely or openly configured ground floor and the uniformly infilled upper stories. Under the June 24, 2026 foreshock-mainshock sequence, seismic lateral forces were initially resisted by the stiffer infill-frame system at the ground level. As infill panels reached their in-plane shear capacity, diagonal cracking propagated and stiffness degraded rapidly, shifting lateral deformation demand to the bare RC frame columns. Simultaneously, out-of-plane inertial demands expelled brick units from frame bays, eliminating residual lateral resistance and exposing the RC frame to increased drift demand. The RC frame columns appear to have sustained this demand without primary structural collapse — preserving life safety for occupants in the upper stories — while the ground-story nonstructural and infill systems experienced extensive nonstructural and infill failure. The foreshock-mainshock sequence compounded this process by pre-damaging the ground-story infill prior to peak seismic demand.

This hypothesis is consistent with the vertically distributed damage gradient documented in Section 3, the structural mechanics described in Section 4, and the failure typology classified under ASCE 41-17 as soft-story collapse mechanism with unreinforced masonry infill participation (ASCE 2017).

Table 5: Summary of Contributing Factors, Engineering References, and Evidence Basis for Observed Failure Mechanisms

Contributing Factor	Code Reference	Evidence Basis	Confidence
Vertical stiffness discontinuity	ASCE 7-22 § 12.3.2.2 (ASCE 2022)	Vertical damage gradient - Section 3	High*
No infill-frame gap detailing	FEMA 306 / ASCE 41-17 (FEMA 1998; ASCE 2017)	Brittle failure pattern - Sections 3 & 4.3	Moderate*
Unreinforced masonry infill (URM)	ACI 318-19 / FEMA 306 (ACI 2019; FEMA 1998)	Exposed brick — no reinforcement visible	High
Foreshock-mainshock pre-damage	Seismic sequence record (USGS 2026; VERT 2026)	M7.2 + M7.5 event documentation	High
Drift limit exceedance	ASCE 7-22 §12.12.1 (ASCE 2022)	Near-total infill failure - ground level	High
Non-structural MEP vulnerability	ASCE 7-22 Ch. 13 (ASCE 2022)	MEP damage at ground level	Moderate

*Confidence levels in Table 5 represent the strength of engineering support for each interpretation based on the available evidence. These qualitative ratings reflect the consistency between the observed damage and established structural behavior and are not intended to represent statistical confidence.

High: Directly supported by visible evidence and consistent with established engineering principles or code-based behavior.
Moderate: Reasonably supported by the available evidence and consistent with established structural mechanics, although direct confirmation is unavailable.
Low: Based primarily on engineering judgment and plausible structural behavior, with limited direct observational support.

6. Limitations and Scope of Evaluation

The findings and conclusions presented in this report are subject to several significant limitations that must be acknowledged in the interest of scientific rigor and engineering integrity.

6.1 Single-Source Visual Evidence

The observational data presented in this report are derived from a single video recording captured by a building occupant during emergency egress. This source, while valuable as a contemporaneous record of post-earthquake conditions, is subject to inherent constraints including camera motion, variable lighting, limited field of view, and the absence of systematic documentation protocol. No independent corroborating visual evidence — such as aerial imagery, post-event field survey photographs, or drone footage — was available to verify or supplement the occupant-captured footage.

6.2 Restricted Observational Scope

Observations are confined exclusively to stairwell enclosures and corridor areas traversed during the occupant's descent. Structural conditions within individual dwelling units, mechanical rooms, the building core, and exterior facade elements could not be assessed. RC frame element conditions — including concrete cracking, reinforcement exposure, and column base behavior — were observable only in limited instances and could not be systematically evaluated. Below-grade conditions were entirely inaccessible due to debris obstruction at the basement stair entry.

6.3 Absence of Structural Documentation

No structural drawings, material specifications, construction records, or geotechnical data were available for this study. Consequently, design-intent lateral force-resisting system configuration, reinforcement detailing, concrete compressive strength, and foundation type remain unknown. The failure hypothesis advanced in Section 5 is based on visual evidence and engineering judgment and cannot be validated against as-built structural parameters.

6.4 Unconfirmed Building Geometry

The total number of stories, floor-to-floor heights, plan dimensions, and structural bay configuration could not be determined from available footage. Floor level designations used throughout this report are approximate and based on the occupant's relative position during descent. The classification of this structure as mid-rise is based on visual evidence of building height relative to surrounding structures and the apparent number of stories traversed during egress, and has not been independently verified.

6.5 Seismic Ground Motion Parameters

Regional USGS ShakeMap ground-motion estimates were available; however, no building-specific instrumental recordings or structural response measurements were available for the investigated structure. The seismic demand imposed on this structure during the June 24, 2026 sequence cannot be quantified from available evidence, precluding any assessment of the correlation between seismic demand intensity and observed damage severity.

6.6 Post-Event Conditions

The video documentation was recorded immediately following the seismic sequence, prior to any post-event intervention. The observed damage states are interpreted as primarily associated with the documented seismic sequence; however, the potential contribution of subsequent aftershocks, human intervention, or time-dependent degradation cannot be independently verified.

Table 6: Summary of Investigation Limitations and Potential Impact on Conclusions

Limitation	Description	Impact on Conclusions
Single-source visual evidence	All observational data are derived from a single occupant-recorded video during emergency egress; no independent photographic, aerial, or field documentation was available.	Limits independent verification of observed damage patterns and failure interpretation.
Restricted observational scope	Documentation is limited primarily to stairwell and corridor areas. Dwelling units, mechanical rooms, structural core elements, exterior façade conditions, and concealed structural members were not systematically evaluated.	Structural conditions outside the documented areas remain unknown.
Absence of	No structural drawings, material	Prevents validation of the

structural documentation	specifications, reinforcement details, construction records, or geotechnical information were available.	failure hypothesis against as-built structural parameters.
Unconfirmed building geometry	Total story count, floor-to-floor heights, plan dimensions, and structural bay configuration could not be independently confirmed.	Story-level damage interpretation and deformation estimates remain approximate.
Unknown exact building location and lack of site-specific ground motion data.	Because the exact geographic location of the investigated building was not disclosed, regional USGS ShakeMap estimates could only provide an overall seismic context. No building-specific instrumental recordings or site-specific ground motion were available.	The quantitative relationship between seismic demand and observed damage severity cannot be established.
Below-grade inaccessibility	Basement and foundation areas were inaccessible due to debris obstruction during filming.	Foundation performance and below-grade structural conditions could not be evaluated.
Post-event sequence uncertainty	Video documentation was captured immediately after the seismic sequence; the individual contribution of the foreshock, mainshock, and possible aftershocks cannot be separated from available evidence.	The timing and progression of individual damage states cannot be independently confirmed.

Consequently, all findings, interpretations, and failure hypotheses presented in this report should be considered preliminary and subject to revision should additional structural, geotechnical, seismic, or photographic documentation become available.

7. Conclusions

This technical case study has examined the vertically distributed seismic damage pattern observed in an RC moment-resisting frame building during the June 24, 2026 Venezuela seismic sequence — comprising a M7.2 foreshock and a M7.5 mainshock — through the analysis of occupant-captured video footage and evaluation using applicable seismic provisions and assessment methodologies from ASCE 7-22, ACI 318-19, ASCE 41-17, and FEMA 306 (ASCE 2017, 2022; ACI 2019; FEMA 1998).

The following conclusions are advanced based on the available evidence:

1. Soft-Story Response Mechanism: The observed damage pattern is consistent with a soft-story collapse mechanism as defined under ASCE 7-22 Section 12.3.2.2 and Table 12.3-1, characterized by the concentration of lateral deformation demand at the ground story and the progressive retention of structural and nonstructural integrity at intermediate and upper levels (ASCE 2022).

2. Masonry Infill Contribution: Unreinforced masonry infill walls appear to have functioned as unintended lateral force-resisting elements prior to failure, introducing stiffness irregularity into the structural system and precipitating brittle in-plane shear and out-of-plane overturning failure modes at the ground level.

3. Primary Frame Stability: The apparent integrity of RC frame elements at the ground level — as observed in video stills — suggests that primary frame collapse did not occur, and that the structure remained within or proximate to the Collapse Prevention performance level for its primary structural system, notwithstanding catastrophic nonstructural failure.

4. Foreshock-Mainshock Sequence Effects: The foreshock-mainshock sequence is identified as a probable amplifying factor, with the M7.2 foreshock likely initiating ground-story infill degradation prior to peak seismic demand imposed by the M7.5 mainshock.

5. Masonry Infill–Frame Interaction: The observed damage pattern demonstrates the potential significance of masonry infill–frame interaction in seismic response evaluation. While current seismic design provisions appropriately address structural safety requirements, structures in which masonry infills substantially influence lateral stiffness may exhibit response characteristics that are not fully represented when infill participation is excluded from analytical models.

6. Seismic Resilience and Recovery Implications: The observed damage pattern demonstrates that seismic resilience extends beyond prevention of global structural collapse and includes the ability of a building to maintain functionality and achieve timely recovery. Although the primary RC frame appears to have maintained global stability based on available visual evidence, extensive ground-story damage to masonry infill and MEP systems would likely increase post-earthquake repair demands, recovery duration, and associated economic impacts. The concentration of damage in vulnerable nonstructural components highlights the importance of resilience-based design strategies that minimize downtime and facilitate rapid restoration of building functionality following major seismic events.

7. Nonstructural Component Performance: The observed damage to mechanical, electrical, and plumbing (MEP) systems indicates that nonstructural component performance represented a critical factor in post-earthquake functionality and recovery. Although the seismic design force provisions of ASCE 7-22 Chapter 13 address inertial demands on nonstructural components, drift-sensitive components such as piping, electrical conduits, and HVAC systems may experience significant damage when subjected to concentrated inter-story deformation demands associated with soft-story response (ASCE 2022). The observed ground-level MEP distress highlights the importance of integrating nonstructural component resilience, anchorage, and deformation compatibility into seismic performance evaluations to reduce downtime and accelerate post-event recovery.

These observations are particularly relevant to resilience-based seismic design approaches in the United States, where reducing post-earthquake downtime and maintaining functionality of critical building systems have become increasingly important objectives.

Table 7: Summary of Principal Conclusions and Engineering Implications

Conclusion Area	Principal Conclusion	Engineering Significance
1. Soft-Story Response Mechanism	The observed vertical damage pattern is consistent with a soft-story response mechanism associated with ground-story stiffness irregularity and concentration of lateral deformation demand.	Highlights the importance of identifying vertical stiffness discontinuities and evaluating potential soft-story vulnerabilities in existing RC buildings.
2. Masonry Infill Contribution	Unreinforced masonry infill walls appear to have contributed to lateral stiffness and strength prior to failure, influencing the seismic response of the RC frame system.	Demonstrates that masonry infills may significantly influence actual structural response even when not included as primary lateral-force-resisting elements.

3. Primary Frame Stability	Available video evidence indicates that global collapse of the primary RC frame did not occur, while severe damage was concentrated in masonry infill and nonstructural components.	Emphasizes the distinction between structural stability, collapse prevention, and post-earthquake functionality.
4. Foreshock-Mainshock Sequence Effects	The M 7.2 foreshock likely contributed to initial ground-story infill cracking and stiffness degradation prior to the M 7.5 mainshock.	Indicates that sequential seismic events may amplify observed damage through cumulative degradation effects.
5. Masonry Infill–Frame Interaction	The observed damage pattern demonstrates the potential significance of infill-frame interaction in seismic response evaluation, particularly where masonry infills substantially influence lateral stiffness.	Supports consideration of infill effects in analytical assessment of existing RC frame buildings where applicable.
6. Seismic Resilience and Recovery Implications	The observed damage demonstrates that seismic resilience extends beyond prevention of global collapse and includes maintaining functionality and reducing recovery duration.	Highlights the importance of resilience-based approaches that address repairability, downtime reduction, and restoration of building functionality.
7. Nonstructural Component Performance	Ground-level MEP damage indicates that drift-sensitive nonstructural components may experience significant damage under concentrated inter-story deformation demands associated with soft-story response.	Reinforces the need for improved anchorage, deformation compatibility, and nonstructural resilience strategies under ASCE 7-22 Chapter 13 provisions (ASCE 2022).

8. Recommendations

The findings of this technical case study provide recommendations for structural engineers, building officials, researchers, and policymakers engaged in post-earthquake assessment, seismic risk reduction, and resilience-based evaluation of reinforced concrete buildings with masonry infill systems.

First, post-event field investigation of the subject structure should be conducted by qualified structural engineering professionals with access to architectural, structural, and below-grade elements to verify the failure mechanisms identified in this study. Detailed evaluation should include assessment of RC frame members, masonry infill conditions, connection details, foundation performance, and residual structural capacity in accordance with applicable assessment procedures such as ASCE 41-17 (ASCE 2017).

Second, existing RC moment-resisting frame buildings with ground-story openness, significant variation in infill distribution, or potential vertical stiffness discontinuities should receive priority consideration during seismic screening programs. Rapid visual screening methods followed, where appropriate, by detailed analytical evaluation can assist in identifying buildings with elevated soft-story vulnerability before major seismic events occur.

Third, seismic evaluation practices for existing reinforced concrete buildings should consider the potential influence of masonry infill-frame interaction where infills substantially modify lateral stiffness, strength, and deformation characteristics. Although masonry infills are commonly treated as nonstructural components in design practice, their contribution to actual seismic response may be significant prior to failure and should be considered where appropriate in analytical assessments of vulnerable building typologies.

Fourth, resilience-based seismic design and assessment approaches should incorporate not only prevention of global structural instability but also reduction of post-earthquake downtime and restoration of building functionality. The observed concentration of damage in masonry infills and MEP systems demonstrates that nonstructural performance can significantly influence repair demands, economic losses, and recovery timelines following major seismic events.

Fifth, drift-sensitive nonstructural components, including mechanical, electrical, and plumbing (MEP) systems, should receive explicit consideration in seismic vulnerability assessments. Appropriate anchorage, flexible connections, seismic bracing, and deformation-compatible detailing should be considered in accordance with ASCE 7-22

Chapter 13 requirements to improve post-earthquake functionality of building systems (ASCE 2022).

Sixth, performance-based seismic evaluation frameworks should continue to advance toward improved representation of actual building response, particularly for existing RC buildings where construction practices, infill configurations, and architectural modifications may introduce behavior not fully captured by simplified analytical assumptions.

Seventh, occupant-recorded video documentation should be recognized as a valuable supplementary source of observational evidence in post-earthquake investigations. Development of standardized procedures for collection, preservation, verification, and analysis of visual evidence — including metadata documentation and chain-of-custody practices — could improve the reliability and reproducibility of future earthquake damage assessments.

Finally, the observations from this case study provide broader implications for seismic risk reduction and resilience-based assessment of existing reinforced concrete buildings in high-seismicity regions. The identified interaction between ground-story stiffness irregularity, masonry infill degradation, and nonstructural system vulnerability represents a recurring challenge for existing reinforced concrete building inventories in earthquake-prone regions. These findings may support continued development of assessment methodologies, retrofit prioritization strategies, and resilience-based practices aimed at reducing post-earthquake downtime and improving recovery of building functionality.

Image Source and Copyright Statement

Conflict of Interest

The authors declare that they have no known competing financial interests or personal relationships that could have appeared to influence the work reported in this technical report.

Ethics Statement

This investigation was conducted exclusively using publicly available observational information. No human participants, personal data collection, laboratory testing, or animal experimentation were involved.

Data Availability Statement

The engineering interpretations presented in this report are based on publicly available video documentation of the June 24, 2026 Venezuela earthquake sequence together with publicly available regional seismic information. Representative image extracts are included in Appendix A. Additional data supporting the findings of this report are available from publicly accessible sources referenced herein.

Funding

No external funding was received for this investigation.

References

1. Agha Beigi, H., Sullivan, T. J., Christopoulos, C., and Calvi, G. M. (2015). "Factors influencing the repair costs of soft-story RC frame buildings and implications for their seismic retrofit." *Engineering Structures,* 101, 233–245. https://doi.org/10.1016/j.engstruct.2015.06.045 .

2. American Concrete Institute. (2019). *Building Code Requirements for Structural Concrete (ACI 318-19) and Commentary*. Farmington Hills, MI.

3. American Society of Civil Engineers. (2017). *Seismic Evaluation and Retrofit of Existing Buildings (ASCE/SEI 41-17)*. Reston, VA.

4. American Society of Civil Engineers. (2022). *Minimum Design Loads and Associated Criteria for Buildings and Other Structures (ASCE/SEI 7-22).* Reston, VA.

5. Basha, S., and Kaushik, H. B. (2016). "Behavior and failure mechanisms of masonry-infilled RC frames (in low-rise buildings) subject to lateral loading." *Engineering Structures*, 123, 1–15. https://doi.org/10.1016/j.engstruct.2015.12.034

6. Crisafulli, F. J. (1997). *Seismic Behaviour of Reinforced Concrete Structures with Masonry Infills*. Ph.D. dissertation, University of Canterbury, Christchurch, New Zealand. https://doi.org/10.26021/1979

7. Dolšek, M., and Fajfar, P. (2008). "The effect of masonry infills on the seismic response of a four-storey reinforced concrete frame—A deterministic assessment." *Engineering Structures*, 30(7), 1991–2001. https://doi.org/10.1016/j.engstruct.2008.01.001

8. Earthquake Engineering Research Institute. (1995). *The Hyogo-ken Nanbu Earthquake, January 17, 1995: Preliminary Reconnaissance Report*. Oakland, CA.

9. Earthquake Engineering Research Institute. (1996). *The Northridge Earthquake of January 17, 1994: Reconnaissance Report*. *Earthquake Spectra,* Supplement C to Volume 11, Parts 1 and 2. Oakland, CA.

10. Federal Emergency Management Agency. (1998). *Evaluation of Earthquake Damaged Concrete and Masonry Wall Buildings: Basic Procedures Manual (FEMA 306)*. Prepared by Applied Technology Council for FEMA, Washington, DC.

11. Federal Emergency Management Agency. (2018). *Seismic Performance Assessment of Buildings, Volume 1 – Methodology (FEMA P-58-1)*. 2nd ed., Washington, DC.

12. Mainstone, R. J. (1971). "On the stiffnesses and strengths of infilled frames." *Proceedings of the Institution of Civil Engineers*, Supplement IV, 2, 57–90. https://doi.org/10.1680/iicep.1971.6267

13. Pallarés, F. J., Davia, A , Hassan, W. M. , Pallarés, L. (2021). "Experimental and analytical assessment of the influence of masonry façade infills on seismic behavior of RC frame buildings." *Engineering Structures*, 243, 112674. https://doi.org/10.1016/j.engstruct.2021.112031

14. Paulay, T., and Priestley, M. J. N. (1992). *Seismic Design of Reinforced Concrete and Masonry Buildings*. John Wiley & Sons, New York.

15. Sleiman, E., Ferrier, E., Michel, L., and Saidi, M. (2024). "Seismic behavior of masonry-infilled reinforced concrete frames strengthened using ultra-high performance concrete diagonal strips." *Structures*, 59, 105790. https://doi.org/10.1016/j.istruc.2023.105790

16. U.S. Geological Survey. (2026). *M7.5 Venezuela Earthquake, June 24, 2026*. Earthquake Hazards Program, U.S. Geological Survey.

17. U.S. Geological Survey. (2026). *ShakeMap: June 24, 2026 Venezuela Earthquake*. Earthquake Hazards Program, U.S. Geological Survey.

18. Virtual Earthquake Reconnaissance Team. (2026). *Phase 1 Response to the M7.2 and M7.5 Venezuela Earthquakes, June 24, 2026*. Earthquake Engineering Research Institute, Oakland, CA. https://learningfromearthquakes.org/wp-content/uploads/2026.06.24-Venezuela-EQ-Phase-1-VERT-Report.pdf

Appendix A: Photographic Evidence

A.1. Overview

Note: The photographs presented in this appendix were extracted from a single occupant-recorded video obtained during the June 24, 2026 earthquake sequence. Image resolution and lighting conditions vary throughout the recording. The photographs have been organized according to the approximate sequence of the occupant's descent and are presented solely as observational evidence supporting the qualitative assessment described in this report.

A.2. Upper Stories

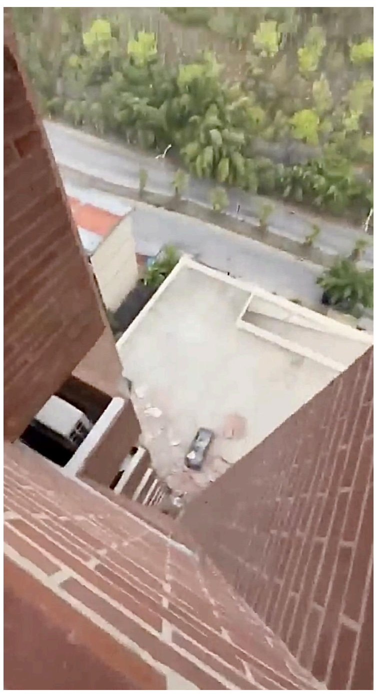

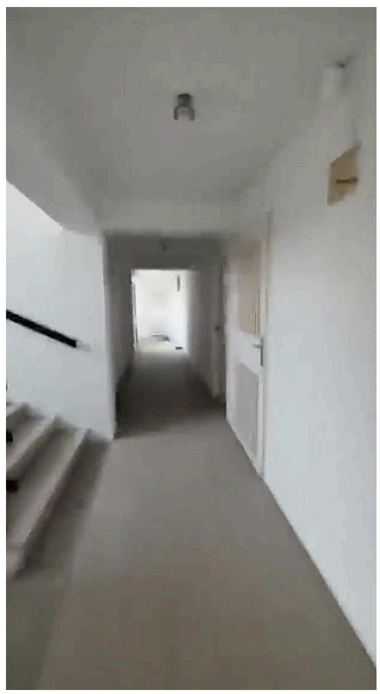

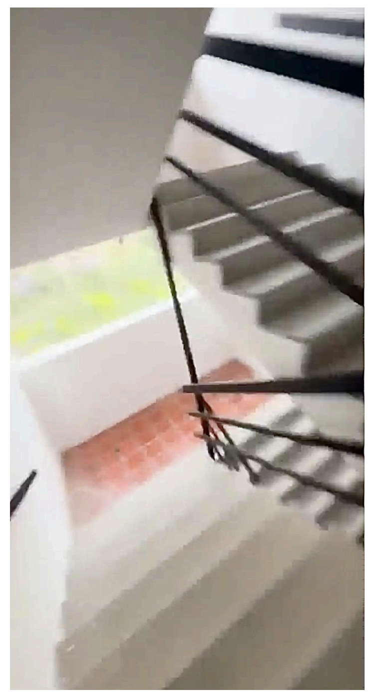

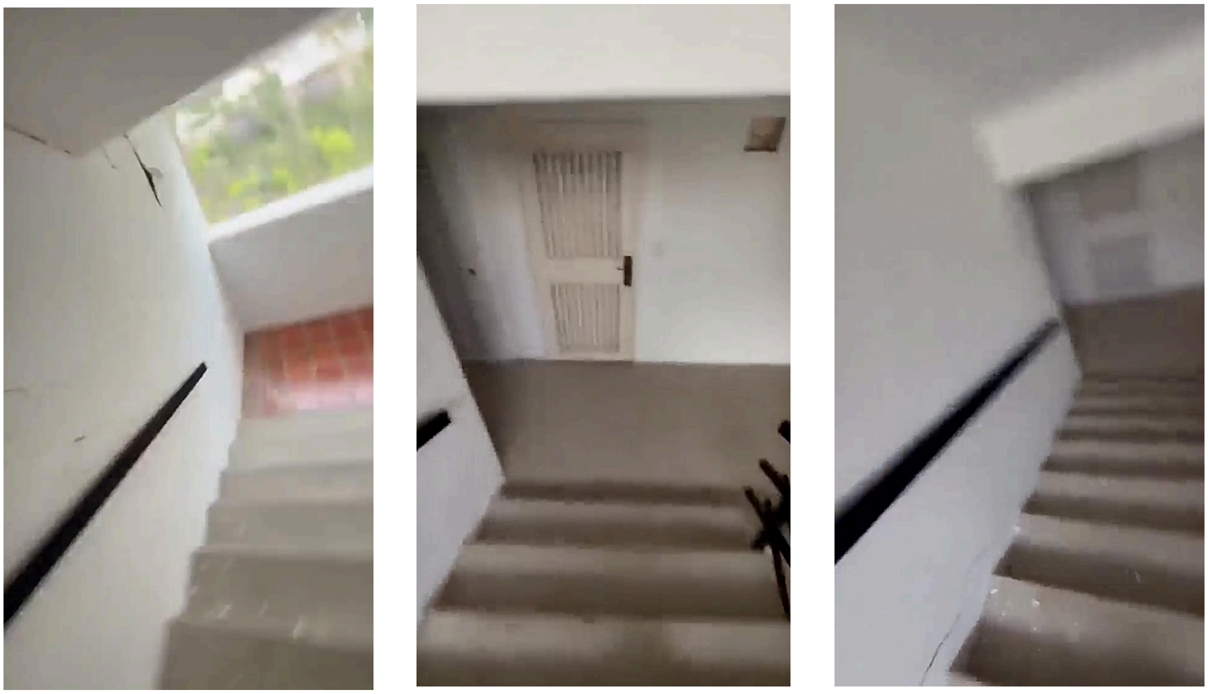

Figure A-2: Representative visual observations from the upper stories. The observed conditions are generally consistent with damage characteristics commonly associated with the Immediate Occupancy (IO) performance level defined in ASCE/SEI 41-17: (a) exterior view showing intact brick masonry; (b) corridor with intact wall finishes and floor surfaces free of visible debris; (c) unobstructed stairwell enclosure; (d) stairwell view showing a single hairline crack at the wall-to-slab interface; (e) door frames appearing plumb, with no visible evidence of significant distortion; and (f) stairwell landing free of visible debris accumulation

A.3. Intermediate Stories



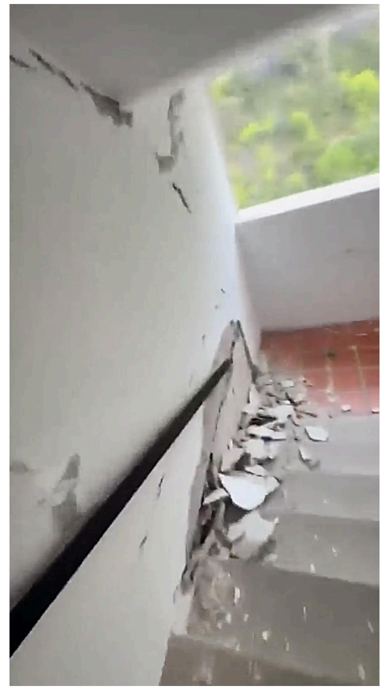


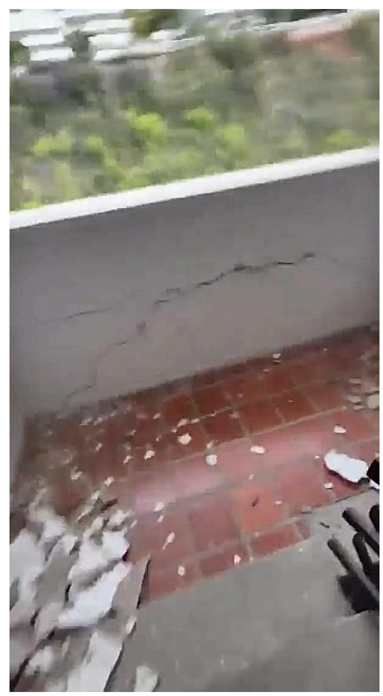

Figure A-3: Representative visual observations from the intermediate stories. The observed conditions indicate a progressive increase in damage severity compared to the upper stories, generally consistent with damage characteristics commonly associated with the Life Safety (LS) performance level defined in ASCE/SEI 41-17: (a) diagonal cracking and plaster spalling at stairwell landing walls, exposing the underlying masonry infill; (b) close-up view of extensive diagonal shear cracking in the masonry infill wall; (c) significant accumulation of masonry debris on stair treads and the landing; (d) view from the intermediate landing showing progressive cracking of the stairwell enclosure walls; (e) minor racking distortion visible at the corners of the door frame; (f) overall view of the stairwell illustrating the downward progression of damage; (g) increased accumulation of masonry debris on the stair treads; (h) corridor with accumulation of masonry debris; and (i) significant plaster spalling exposing the underlying masonry infill, accompanied by substantial accumulation of debris on the stairway.

A.4. Lower Stories

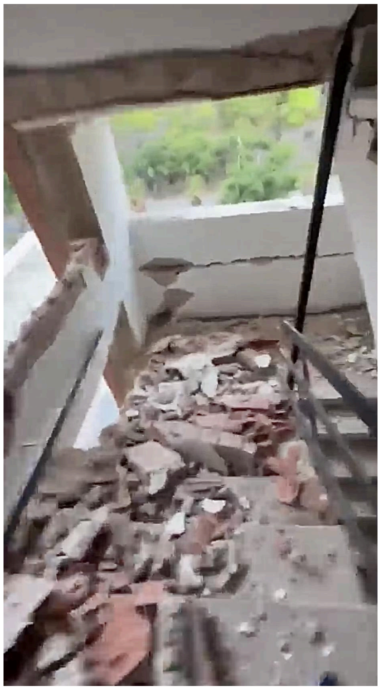
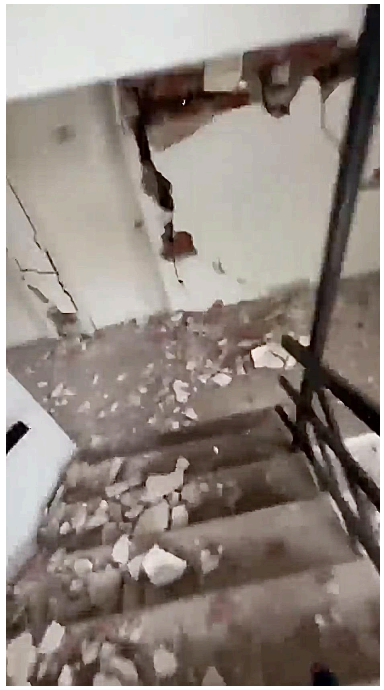
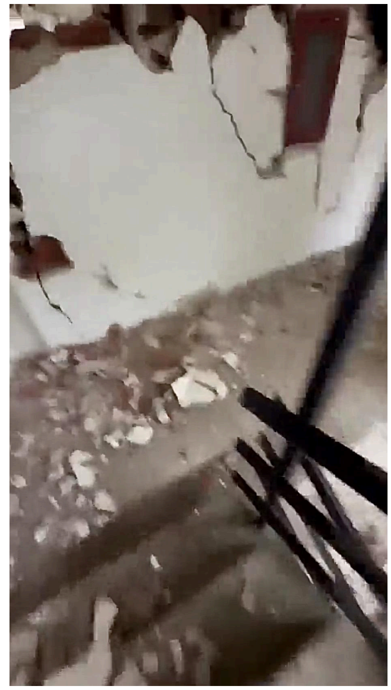


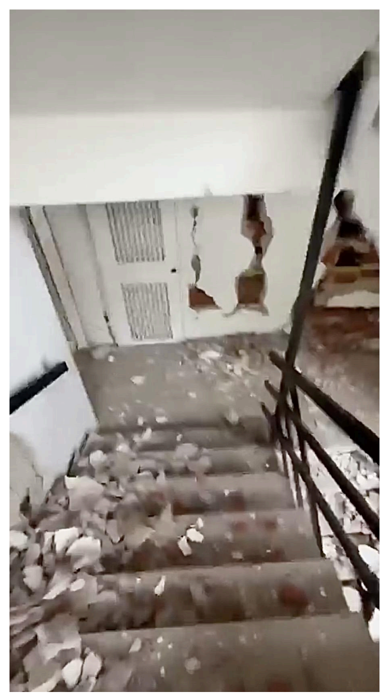

Figure A-4: Representative visual observations from the lower stories. The observed conditions demonstrate a pronounced escalation in damage severity compared to intermediate stories, generally consistent with severe nonstructural and infill damage approaching conditions associated with the Collapse Prevention (CP) performance level defined in ASCE/SEI 41-17: (a) Extensive collapse and loss of continuity of unreinforced masonry (URM) infill walls within the stairwell enclosure, with large portions of wall panels no longer intact; (b) and (c) wide vertical separation cracks within the corridor masonry infill walls, likely associated with seismic-induced incompatibility between the lateral deformation demands of the structural frame and the brittle response of the URM infill panels. Progressive frame–infill separation, combined with out-of-plane instability and localized dislodgement of masonry units, resulted in significant degradation of infill wall integrity, accompanied by cracking around door openings and separation between infill walls and surrounding frame elements; (d) extensive failure of stairwell enclosure walls with progressive loss of wall continuity across multiple stories, exposing exterior openings and adjacent building spaces; (e) widespread cracking, spalling, and partial detachment of masonry infill and finish materials at the lower levels; (f) similar conditions to those observed in (a) and (b), including severe deterioration and loss of continuity of URM infill walls; (g) complete failure of portions of the stairwell enclosure walls, resulting in significant loss of enclosure integrity; (h) substantial accumulation of masonry debris obstructing stair treads and landing slabs, limiting accessibility and indicating severe localized infill failure; and (i) conditions similar to those described in (a), showing extensive collapse and loss of continuity of URM infill wall panels.

A.5. Ground Level

Figure A-5: Representative visual observations from the ground level. The observed conditions document the most severe damage encountered during the survey, characterized by extensive failure of unreinforced masonry infill walls consistent with apparent soft-story response mechanisms, while visible

RC frame members generally retained geometric alignment. Conditions approach damage states associated with the Collapse Prevention (CP) performance level defined in ASCE/SEI 41-17 for nonstructural components: (a) heavy debris blocking access to basement stairs; (b) extensive dispersion of masonry units and collapsed nonstructural partitions in the corridor; (c) heavy structural debris obstruction, and standing water from damaged MEP utilities; (d) and (e) overall view of lobby showing significant structural and nonstructural damage indicating potential soft-story behavior and (f) view towards exterior showing collapsed infill